Effect of Friction and Cohesion on Anisotropy in Quasi-static Granular Materials under Shear

A. Singh, V. Magnanimo and S. Luding

Multi Scale Mechanics, CTW, MESA+, UTwente P.O.Box 217, 7500 AE Enschede, Netherlands

Abstract. We study the effect of particle friction and cohesion on the steady-state shear stress and the contact anisotropy of a granular assembly sheared in a split-bottom ring shear cell. For non-cohesive frictional materials, the critical state shear stress first increases and then saturates with friction. The contact number density is found to decrease monotonically, while the anisotropy of the contact network saturates after an initial increase. For cohesive powders, the relation between shear stress and confining pressure becomes non-linear. Interestingly the contact number density stays almost unaffected, while the structural anisotropy decreases with increasing cohesion, hinting at a redistribution of the network with almost constant contact number density.

Keywords: Friction, anisotropy, fabric, macroscopic friction.
PACS: PACS: 45.70.Cc, 83.80.Fg, 81.20.Ev

INTRODUCTION

What do sand, rice, coffee and cocoa powder have in common? They all are *granular materials*: a collection of non-Brownian, macroscopic particles with dissipative interactions. The intrinsic nonlinear and dissipative nature of their interactions lead to a great deal of interesting phenomena like segregation, jamming, clustering, and shear-band formation. Many of these macroscopic phenomena find their origin in the kinematics at lower scale. The Discrete Element Method (DEM) is a recently established powerful tool to investigate the micromechanics of a granular material. The method involves the numerical solution of Newton's equations of motion, based on specific particle properties and interaction laws [1].

One current research goal in this field is to describe the macroscopic continuum behavior in terms of given micromechanical properties. Finding a connection between the two scales involves the so-called micro-macro transition [2, 3]. From local averaging over adequate representative volume elements (RVE)s – inside which all particles are assumed to behave similarly – one can obtain local continuum relations [4, 5, 6]. In this study both local spatio- and temporal-averaging are applied for a (presumed) steady state in the case of a ring-shear cell with split bottom. The split induces a shear-rate gradient and hence a shearband into the system. Due to the weight of the material, a wide range of confining pressures, densities and shear-rates can be scanned and local constitutive relations can be obtained from a single simulation. We focus on the effect of particle contact properties (contact friction and contact adhesion/cohesion) on the steady state macroscopic properties of the system. After introducing DEM, the system and the parameters, we study the pressure, the deviatoric stress, the contact number density, and the structural/contact anisotropy.

MODEL SYSTEM GEOMETRY

Split-bottom ring shear cell. The geometry of the system is described in detail in Refs. [5, 7, 8, 9, 10]. An assembly of spherical beads is confined between two concentric cylinders with gravity, with a free top surface. The concentric cylinders rotate relative to each other around the symmetry axis. The ring shaped split at the bottom separates the moving and static part of the system. Due to the split, a stable shear band appears at the bottom and its width considerably increases from bottom to top ([8] and references therein).

Material parameters. The system is filled with $N \approx 37000$ spherical particles with density $\rho = 2000\,\mathrm{kg/m^3} = 2\,\mathrm{g/cm^3}$. The average size of particles is $a_0 = 1.1\,\mathrm{mm}$, with a homogeneous size-distribution of the width $1 - \mathscr{A} = 1 - \langle a\rangle^2/\langle a^2\rangle = 0.18922$ (with $a_{\min}/a_{\max} = 1/2$). A linear contact model is used to describe the interaction between particles with contact stiffness $k = 100\,\mathrm{Nm^{-1}}$. The rolling and torsion friction are inactive, i.e. $\mu_r = 0.0$ and $\mu_o = 0.0$. The normal and tangential viscosities are $\gamma_n = 0.002\,\mathrm{kg\,s^{-1}}$ and $\gamma_t/\gamma_n = 1/4$. In order to study the influence of contact friction, we use the following set of friction coefficients: $\mu_\mathrm{p} = [0.0, 0.01, 0.02, 0.05, 0.1, 0.2, 0.5, 1.0, 2.0]$. In the other hand, we want to analyze the effect of contact adhesion/cohesion, that is we adopt an adhesive elasto-plastic contact model [4] involving an elastic limit stiffness $k_2 = 500\,\mathrm{Nm^{-1}}$, a plastic stiffness $k_1 = 100\,\mathrm{Nm^{-1}}$, and an ad-

Powders and Grains 2013
AIP Conf. Proc. 1542, 682-685 (2013); doi: 10.1063/1.4812023

hesive "stiffness" k_c. The simulations are run for different values of the non-dimensional adhesive strength (as defined in [11]) $\beta = k_c/k_1 = [0, 0.1, 1]$, while the particle friction is set to $\mu_p = 0.01$.

Since we are interested in the quasi-static regime, the rotation rate is chosen such that the kinetic energy supplied by rotation is negligible compared to the work done by internal stress per unit time and unit mass. The quasi-static limit is then characterized by the condition that the energy ratio, i.e. the inertial number [12], is much smaller than unity, with the rotation rate $f_o = 0.01\,\mathrm{s}^{-1}$ satisfying the condition. The simulation runs for 120 s. For spatial and time averaging, only large times are taken into account, disregarding the transient behavior at the onset of shear.

Averaging and micro-macro procedure. Cylindrical translational invariance is assumed in the tangential ϕ direction, and the averaging is performed over toroidal volumes, over many snapshots in time (typically 40 – 60 s). This leads to fields $Q(r,z)$ defined in terms of radial and vertical positions (r,z) [5, 7]. From the simulations, one can calculate the stress tensor as $\sigma_{ij} = \frac{1}{V}\left[\sum_{p\in V} m^p (v_i{}^p)(v_j{}^p) - \sum_{c\in V} r_i{}^c f_j{}^c\right]$ with particles p, contacts c, mass m^p, velocity v^p, force f^c and branch vector r^c. The first term is the sum of kinetic energy fluctuations, and the second involves the dyadic product of the contact-force with the contact-branch vector. For the small rotation rate f_o used in the following, the contribution of kinetic stress is small compared to the contact stress, hence the former is ignored.

The quantity which describes the local configuration of a granular assembly is the fabric tensor [13], $F_{ij} = \frac{1}{V}\sum_{p\in V} V^p \sum_{c\in p} n_i{}^c n_j{}^c$, where V^p is the particle volume which lies inside the averaging volume V, n^c is the normal unit branch-vector pointing from center of particle p to contact c.

For both stress and fabric tensors, we can calculate the eigenvalues and define the volumetric part $Q_\mathrm{v} = (Q_1+Q_2+Q_3)/3$ and the deviatoric magnitude as $Q_\mathrm{dev} = \sqrt{((Q_1-Q_2)^2+(Q_2-Q_3)^2+(Q_3-Q_1)^2)/6}$. The isotropic/volumetric stress is the confining pressure p and σ_dev, i.e. the second invariant of stress, is used to quantify the deviatoric stress (i.e. the "anisotropy of stress"). The volumetric fabric F_v represents the contact number density, while the deviatoric fabric F_dev quantifies the anisotropy of the contact network. Due to the geometry, the strain-rate tensor is defined by $\dot\varepsilon_\mathrm{v} = 0$ and $\dot\varepsilon_\mathrm{dev} = \dot\gamma$, with the (simple) shear rate $\dot\gamma$, in the shear plane with orientation as described in Refs. [5, 7].

RESULTS

For a given confining stress (and preparation history), the material can only resist shear up to a certain deviatoric (shear) stress, called the "yield stress", beyond which it fails [6, 14]. When yield points $(p^{(y)}, \sigma^{(y)}{}_\mathrm{dev})$ are collected in the $\sigma_\mathrm{dev} - p$-plane, a yield locus can be identified, that fully describes the failure behavior of the material, i.e. its transition from static to dynamic state. In addition, when the material is sheared continuously for a long time, it reaches a steady state which is characterized by a steady state yield stress, i.e. the stress needed to keep the material in motion, $(p^{(c)}, \sigma^{(c)}{}_\mathrm{dev})$, also referred to as the critical state or "termination locus". For simple non-cohesive granular materials, the termination locus can be predicted from a Coulomb type criterion as a straight line with a slope that can be called the (critical) steady state macroscopic friction coefficient $\mu_\mathrm{macro} = (\sigma^{(c)}{}_\mathrm{dev})/p^{(c)}$. When adhesion/cohesion is introduced at the contacts, a more complicated picture appears as described in Ref. [6] and discussed below.

When the material fails, shear strain gets localized in a shearband that, in case of the split-bottom cell, is stable, rather wide with error-function shape, and develops far from the walls. In order to identify the shearband, we only consider data with local shear rate above a given threshold $\dot\gamma^*$. Based on [5, 6, 7], we choose $\dot\gamma^* = 0.08\,\mathrm{s}^{-1}$

Effect of particle friction. In Fig. 1, we plot the macroscopic friction coefficient μ_macro against the contact friction coefficient μ_p. For $\mu_\mathrm{p} = 0$, one observes μ_macro non-zero due to interlocking between particles. μ_macro increases rapidly and reaches an asymptote at high μ_p, possibly dropping for $\mu_\mathrm{p} > 1$ (which has to be studied in more detail). In the inset we plot the shear stress σ_dev against p, that shows a Coulomb-type linear relation, the slope of which provides μ_macro.

In Fig. 2 we plot the volumetric fabric against pressure. For a given μ_p, F_v slightly increases with pressure (an interesting small drop is observed at the highest pressure level). On the other hand, F_v decreases with increasing μ_p, as a single particle needs less contacts to be in mechanical equilibrium with higher contact friction.

Fig. 3 shows the deviatoric fabric F_dev plotted against pressure p. Opposite to the volumetric component, the fabric anisotropy increases with contact friction. That can be related to the decrease in F_v: As the packing becomes looser anisotropy becomes stronger. Upon shearing the probability of particle contacts to establish in favorable directions is higher due to presence of empty voids in systems with larger μ_p. Both F_v and F_dev, below their strong fluctuations, display a change in behavior with increasing contact friction coefficients. In the case of small μ_p a more pronounced increase with pressure shows up, while for large μ_p both F_v and F_dev seem

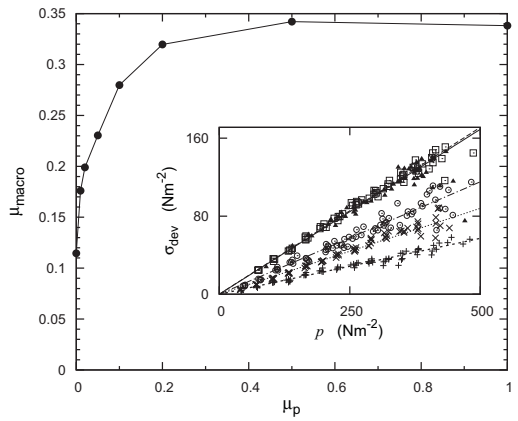

FIGURE 1. Macroscopic friction coefficient plotted as function of particle friction coefficient. The inset shows deviatoric (shear) stress $\sigma_{\rm dev}$ plotted against pressure p. The different symbols correspond to simulations using different particle friction coefficients $+(\mu_{\rm p}=0)$, x$(\mu_{\rm p}=0.01)$, o$(\mu_{\rm p}=0.05)$, $\Box(\mu_{\rm p}=0.5)$ and $\blacktriangle(\mu_{\rm p}=1.0)$.

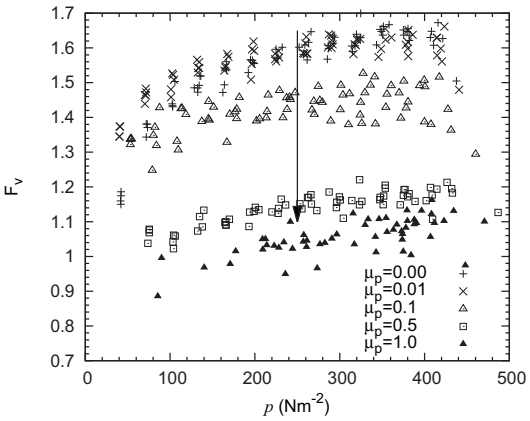

FIGURE 2. Volumetric fabric $F_{\rm v}$ plotted against pressure p. The different symbols correspond to data from simulations with different particle friction coefficients, as given in the inset.

to vary little with pressure (quantifying this is subject of present research with better statistics). We speculate on the origin of this behavior by assuming that less redistributions in the contact network are taking place in the case of high friction rather than low friction, since in the former case the number of contacts (in each direction) stays closer to the allowed minimum, irrespective of the confining pressure.

Effect of cohesion. In Fig. 4 we plot the deviatoric stress $\sigma_{\rm dev}$ against pressure p for different cohesive-

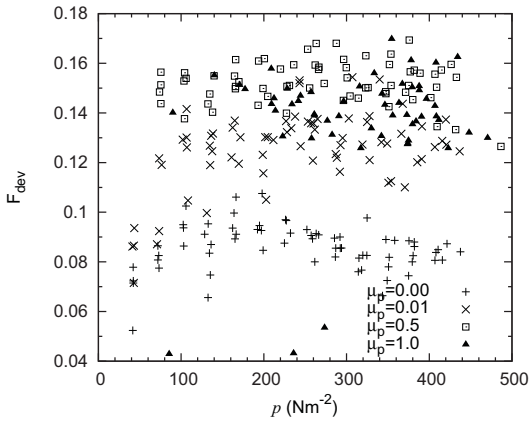

FIGURE 3. Deviatoric fabric $F_{\rm dev}$ plotted against pressure p. The different symbols correspond to simulations using different particle friction coefficients, as given in the inset.

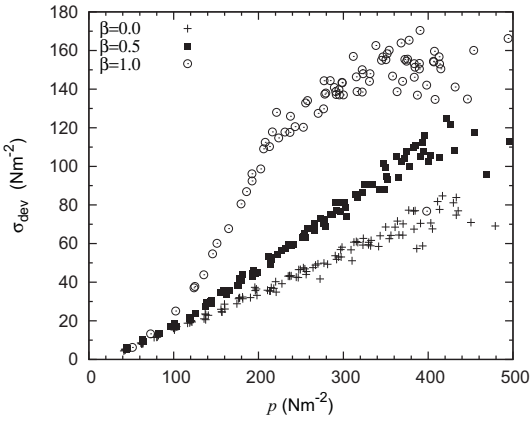

FIGURE 4. Shear stress $\sigma_{\rm dev}$ plotted against pressure p. Different symbols correspond to simulations using different particle cohesion parameters β, as given in the inset.

strengths β. With increasing β, the relation between $\sigma_{\rm dev}$ and p (Coulomb termination locus) becomes non-linear, as studied in more detail in Ref. [6].

Here we focus on the effect of particle cohesion on fabric. The simulation data collapse when the volumetric component $F_{\rm v}$ is plotted against p for different β (not shown), since the contact cohesion strength does not affect the constraints as friction does. A different behavior appears when we plot $F_{\rm dev}$ against p in Fig. 5. The non-cohesive case ($\beta=0$) is identical to the previous frictional analysis. Interestingly, for the intermediate $\beta=0.5$, $F_{\rm dev}$ is found to decrease with increasing p: With higher cohesion and pressure, contacts redistribute more isotropically even though the total number of con-

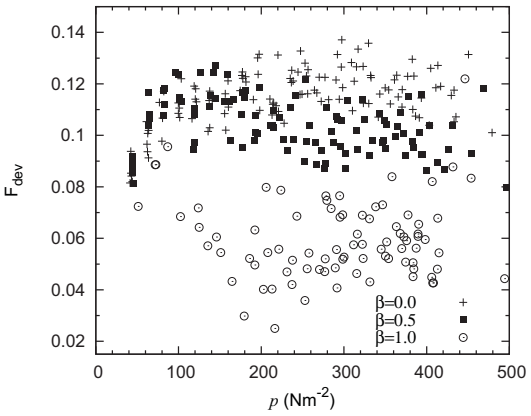

FIGURE 5. Deviatoric fabric F_{dev} plotted against pressure p. Different symbols correspond to simulations using different particle cohesion parameters β, as given in the inset.

tacts remains almost unaffected. Finally, for the strongest cohesion $\beta = 1.0$, F_{dev} first decreases with pressure and later a slight increase/saturation trend is observed (within large fluctuations, as has to be studied in more detail). For cohesive particles, the strength of the adhesive contact force is pressure dependent [6] and so is the probability of loosing a contact or building up a new contact. With increasing cohesion, the particles have the tendency to stick and stay together, hence less contacts are lost in the tensile direction. Contacts in the compressive direction redistribute in order to balance or compensate the tensile contacts, which leads to an overall decrease of fabric anisotropy.

DISCUSSION

The effect of micromechanical parameters on the macroscopic rheological properties of a granular material have been studied by means of the discrete element method (DEM). Different features have been highlighted, when varying contact friction and cohesion. The termination locus (critical state shear/deviatoric stress) is a linear function of pressure, as predicted by the Mohr-Coulomb criterion, with the macroscopic friction increasing with contact friction – in non-cohesive materials. It gets non-linear when cohesion is introduced at the contacts.

The contact network is affected by increasing friction in its volumetric (isotropic) part, due to the reduced minimum number of contacts needed for mechanical equilibrium; but it is not much affected by cohesion. On the other hand, both friction and cohesion affect the orientation of contacts in space and thus the structural anisotropy. Similarities between the deviatoric components of stress and fabric appear for both frictional and cohesive materials: F_{dev} and σ_{dev} saturate for high contact friction, and non-linearity comes into picture once cohesion is introduced, but – in contrast to the increasing deviatoric stress – the structural anisotropy decreases with cohesion.

Acknowledgments Financial support through the "Jamming and Rheology" project of the Stichting voor Fundamenteel Onderzoek der Materie (FOM), which is financially supported by the "Nederlandse Organisatie voor Wetenschappelijk Onderzoek" (NWO), is acknowledged.

REFERENCES

1. M. P. Allen and D. J. Tildesley. *Computer Simulation of Liquids*. Oxford University Press, Oxford, 1987.
2. P. A. Vermeer, S. Diebels, W. Ehlers, H. J. Herrmann, S. Luding, and E. Ramm, editors. *Continuous and Discontinuous Modelling of Cohesive Frictional Materials*, Berlin, 2001. Springer. Lect. Not. Phys. 568.
3. M. Lätzel, S. Luding, and H. J. Herrmann. *Gran. Matt.*, 2 (3):123–135, 2000.
4. S. Luding. *Gran. Matt.*, 10:235–246, 2008.
5. S. Luding. *Particulate Science and Technology*, 26(1): 33–42, 2008.
6. S. Luding and F. Alonso-Marroquín. *Gran. Matt.*, 13: 109–119, 2011.
7. S. Luding. *Particuology*, 6(6):501–505, 2008.
8. J. A. Dijksman and M. van Hecke. *Soft Matter*, 6: 2901–2907, 2010.
9. D. Fenistein, J. W. van de Meent, and M. van Hecke. *Phys. Rev. Lett.*, 92:094301, 2004.
10. D. Fenistein and M. van Hecke. *Nature*, 425(6955):256, 2003.
11. A. Singh, V. Magnanimo, and S. Luding. Sticking of cohesive particles in elasto-plastic collision. subm., 2012.
12. F. da Cruz, S. Emam, M. Prochnow, J. J. Roux, and F. Chevoir. *Phys. Rev. E*, 72:021309, Aug 2005.
13. M. Oda, K. Iwashita, and H. Kazama. Micro-structure developed in shear bands of dense granular soils and its computer simulation – mechanism of dilatancy and failure. In N. A. Fleck and A. C. E. Cocks, editors, *IUTAM Symp. Mech. Gran. Porous Mat*, pages 353–364. Kluwer Academic Publishers, 1997.
14. J. Schwedes. *Granular Matter*, 5(1):1–45, 2003.